Lab 4: Locust Olfaction

Pranav Maddula

Lab Partners: Bryce Maxwell, Andrew Whitaker

Washington University in St. Louis

BME 301A

Lab Instructor: P. Widder

Experiment date: 11/1/19

Submission Date: 11/12/19

I hereby certify that this report is my own original work: **Pranav Maddula**

Introduction:

Olfaction is a complex topic in biomedical engineering that is relatively unexplored. However, olfaction plays a large part in the sensory experience of humans and has immense potential for advancing the field of sensor design. This lab aims to teach the basics of generating and analyzing olfaction data in the model organism, locusts. The concepts behind Electroantennography and data modeling and prediction of complex biological data are emphasized in the lab. Students also continue to build on the concepts taught in previous labs, namely the analysis of signals recorded from complex biological systems, an understanding of modern biomedical instrumentation, and building effective technical communication skills.

As mentioned, the olfaction concepts covered in this lab have immense potential uses in numerous applications. From sensor design to disease diagnosis and bomb detection, olfaction can play a key role in solving many complex problems in a simple and elegant way. For example, the Raman Lab has been given $750,000 from the Office of Naval Research to design and build bomb detectors using the olfactory system of locusts as sensors (Lugo). Likewise, multiple groups are working on detecting cancer via breath analysis. This is done by measuring the amount and ratios of certain volatile organic compounds (VOCs) and using these as a predictor and diagnosis tool for certain cancers (Amor et al.). Likewise, lots of research is going into the design and production of bio-inspired sensors. From infrared sensors based on pit vipers to electronic noses based on dogs, there are boundless potential opportunities for improvement in sensor technology inspired by biology (Wolf).

Methods:

The setup for this lab has three distinct sections; odor and air system, electrical and LabChart, and locust dissection. Following the procedure for the air filter construction in the PLab manual, connect the pump, tubing, filter, and the odor bottles as described in **Figure 6.13** of the PLab manual. Next, connect the power supply to the breadboard and wire up the pump power leads to the button on the breadboard. Afterward, attach leads to channels 1 & 2 of the PowerLab and connect the channel two leads across the button. Following this, power up the PowerLab device and ensure that it is detected by the PC. Following this, set up the recording in LabChart by reducing the scale of channel 1 to 10mv, and increasing the scale of channel 2 to 10v. Next, set up the testing chamber under the ring stand. Place saline in both wells of the antenna stage and ensure the silver electrodes are coated properly and placed in the wells. Attach the channel 1 leads to the silver electrodes. Ensure that all of the connections are made and that the experimental setup thus far fully conforms to **Figure 6.13** of the PLab manual. Finally, acquire a locust and use the dissection scissors to snip off an antenna at both ends. Place the antenna on the stage and ensure that both snipped ends are in the saline wells. Note that as time passes, the antenna gets progressively less and less sensitive as it slowly dies.

For the testing on the locust antenna, various frequencies of odor pulses were administered, and the electroantennogram (EAG) data was recorded. The EAG measures the voltage across the antenna, which can be used as a proxy for olfactory receptor neurons (ORN) activity in the antenna. For this lab, the following pulse frequencies were used; a singular 4-second pulse, a train of 10 1-second pulses with a 2-second inter-stimulus interval (ISI), a train of 10 1-second pulses with a 1-second ISI, a train of 10 1-second pulses with a 500-millisecond ISI, and a train of 10 1-second pulses with a 250-millisecond ISI. Finally, a random series of pulses is given. This procedure should be completed for each of the two odors used, benzaldehyde and hexanol.

Results:

In an attempt to better orient the reader to the nature of the EAG data collected using the methods above, a plot of sample data is provided below.

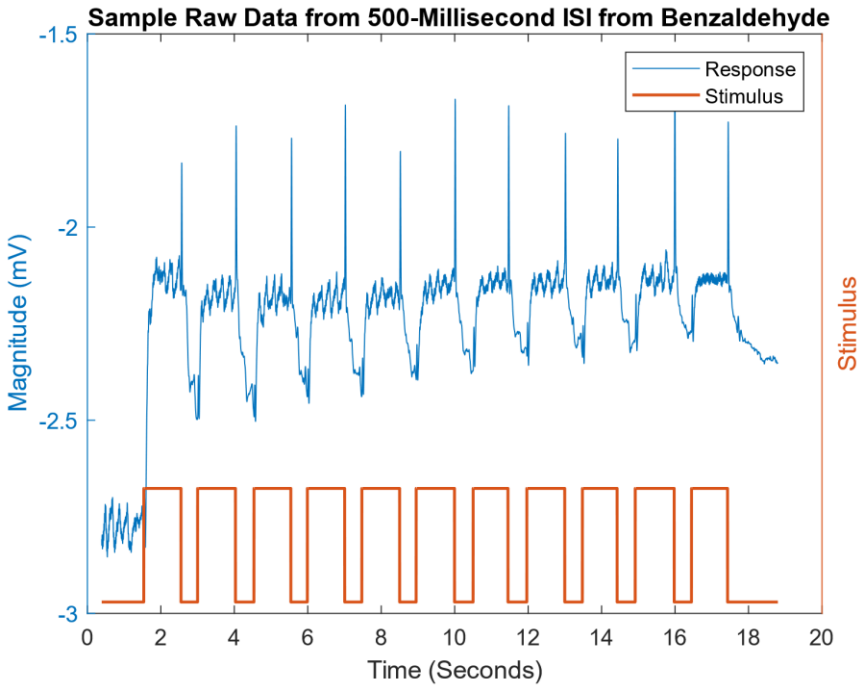

Figure 1: *This figure shows raw EAG data captured from the antenna. The data displayed is across a roughly 18-second time frame. The stimulus is represented in orange, with the high pulses representing on and the zeros representing off. It can be seen that the raw data is extremely noisy.*

From the sample response data, very clear delineations can be seen between the periods of stimulus and periods of no stimulus. This periodicity is used to calculate magnitudes and time constants later on. Additionally, from this distinct periodicity, a high bar of confidence can be drawn from this data, as the data is consistent and easily readable. Additionally, as all of the data used in the lab comes from the sample data, the confidence in the results can be further reinforced. The sample data is used as a very weak EAG response was derived from our experimental data, and no response was seen for hexanol.

Seeing as the raw data is quite hard to work with quantitatively, the recorded EAG response was zero-phase filtered in Matlab using a 200 point window. This step is completed for all data moving forward, and the results for the hexanol ISI are shown below in **Figures 2-5**.

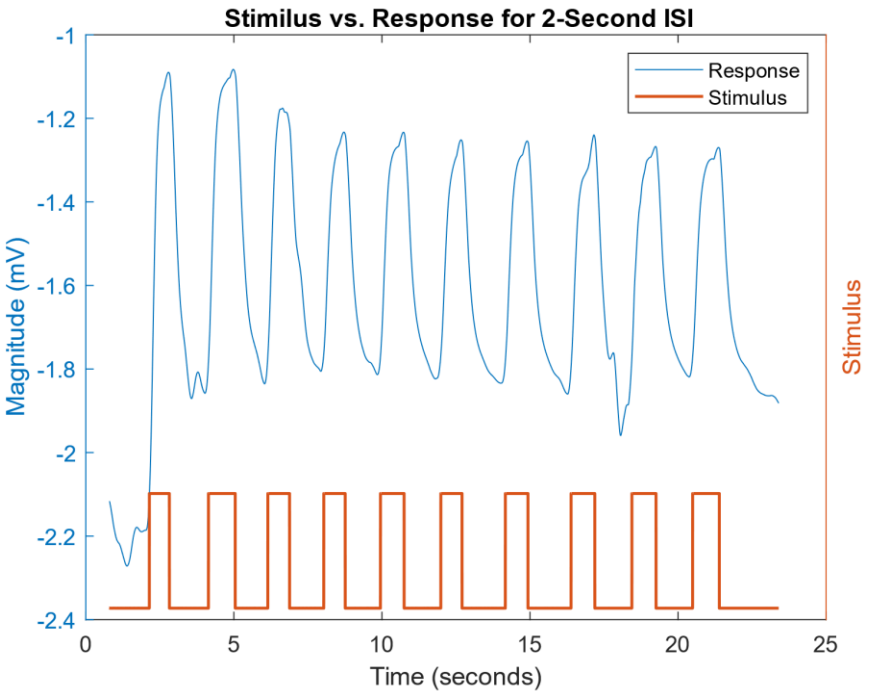

Figure 2: *This figure shows the filtered EAG data for the 2-Second ISI for hexanol. It can be seen that there are large changes in the magnitude of the EAG for on and off signals. The EAG response recorded is in blue, while the stimulus provided is represented in orange.*

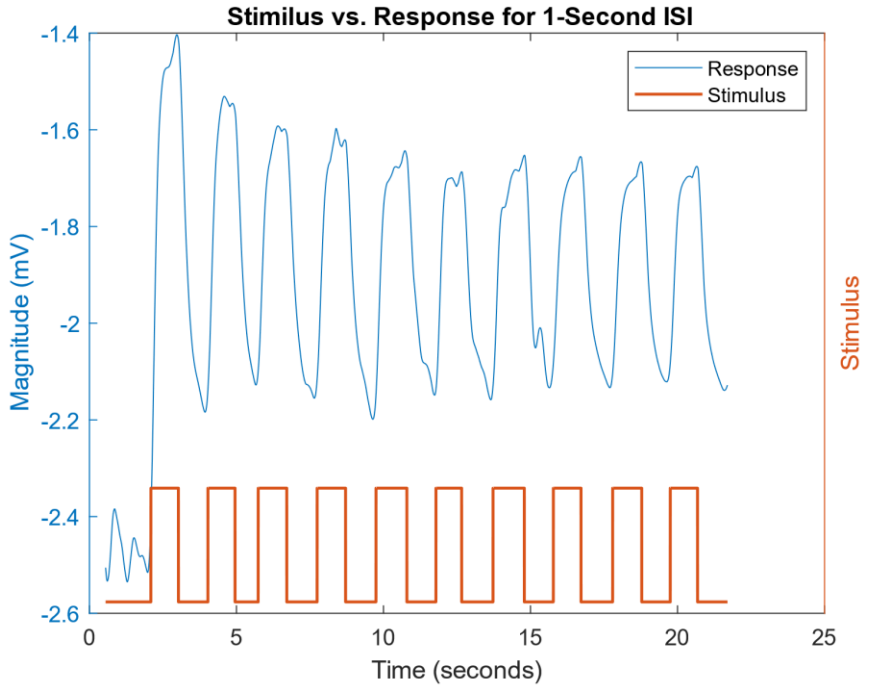

Figure 3: *This figure shows the filtered EAG data for the 1-Second ISI for hexanol. It can be seen that there are large changes in the magnitude of the EAG for on and off signals; however, the magnitude of the change is lower than that of the 2-second ISI.*

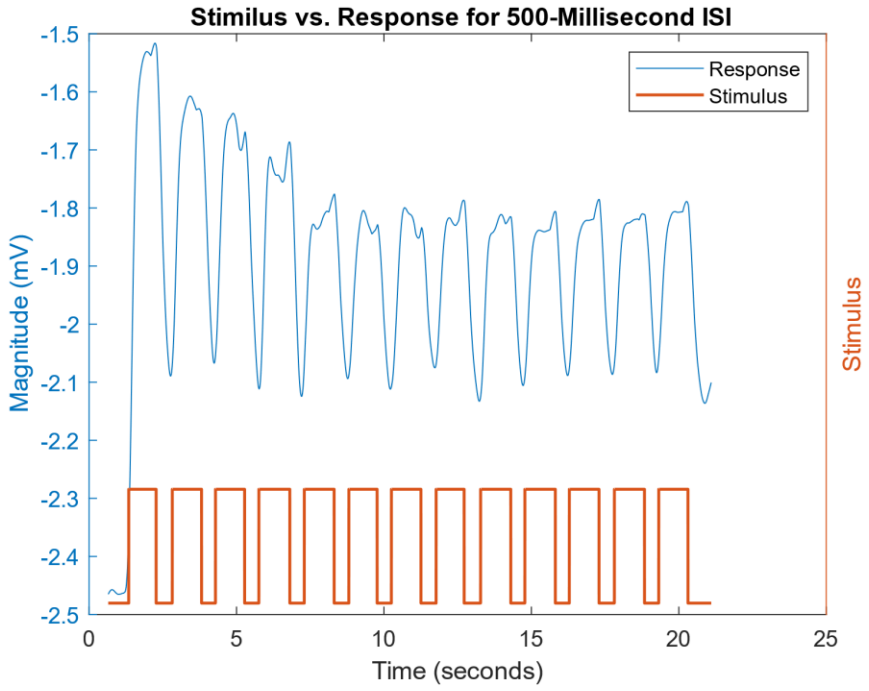

Figure 4: *This figure shows the filtered EAG data for the 500-Millisecond ISI for hexanol. It can be seen that there are large changes in the magnitude of the EAG for on and off signals; however, the magnitude of the change is lower than that of the 1-second ISI. Similarly, the peaks are becoming less well defined.*

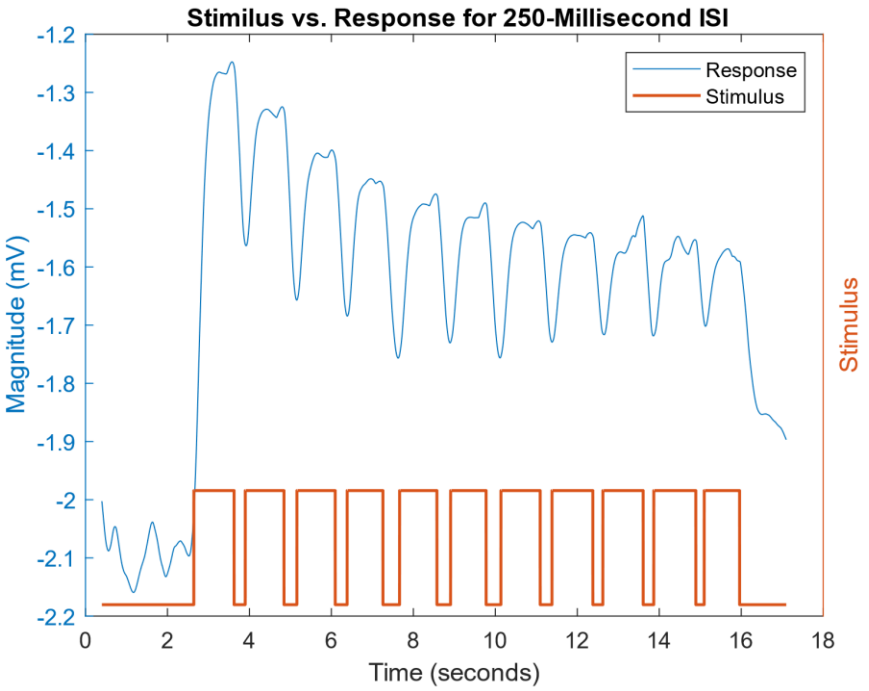

Figure 5: *This figure shows the filtered EAG data for the 250- Millisecond ISI for hexanol. It can be seen that there are large changes in the magnitude of the EAG for on and off signals; however, the magnitude of the change is lower than that of the 500-Millisecond ISI. It can also be seen that as time goes on, the magnitude of the response steadily decreases.*

From this collection of graphs (**Figures 2-5**), it can be seen that as the ISI decreases, the magnitude of the response falls correspondingly. Further, it can also be seen that the magnitude of the response sags as the number of stimulations increases at low ISIs. As mentioned above, this data is pulled from the provided sample data, and thus, there is high confidence in the validity of the data. Moreover, intuitively, the data appears to act as expected in the face of increasing decreasing ISI, with decreasing amplitude and less distinct signals. From these signals, the average amplitude of the periodic portion of the signal for each of the ISI durations for both odors is plotted. The result is as follows:

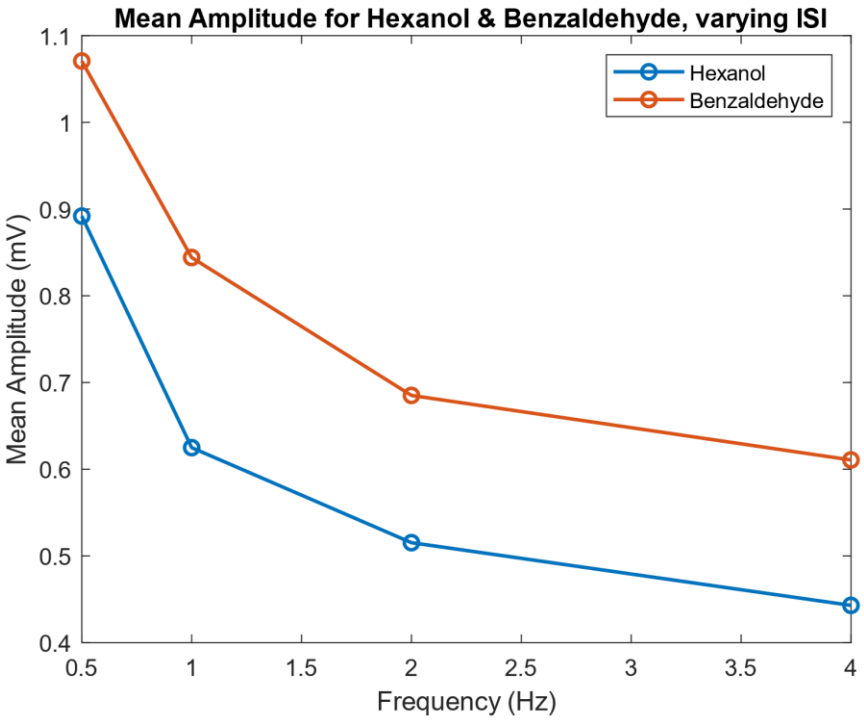

Figure 6: *This figure shows the relationship between the frequency of stimulation (inverse of ISI) and the mean EAG amplitude for the periodic response during the stimulus portion of the data. It can be seen that regardless of ISI, the amplitude of the benzaldehyde response is greater than hexanol. Further, as frequency increases, the mean amplitude decreases*

Seeing these differing frequency response curves for the two odors makes sense, as it would be understandable for the locusts to be more selective towards one odor over the other. One way this selectivity could be expressed is by evoking an increased response in the antenna when exposed to the more preferential odor, as witnessed in the EAG data from **Figure 6**. Digging more deeply into the odor selectivity of the locust, the time constants (rise and fall) for both odors were calculated. The results are as follows:

Rise and Fall Time Constants for Benzaldehyde and Hexanol

	Rise Time	**Fall Time**
Benzaldehyde	.109 Sec	.090 Sec
Hexanol	.154 Sec	.149 Sec

Table 1: *This table shows the calculated rise and fall time constants for benzaldehyde and hexanol. The time constants were calculated to be the time it took to reach 67.2% of the max for the Rise Time and the time it took to drop 32.8% from the max for the Fall Time constant. The Time Constants for both odors was the average of three trials, from the 4-second long odor pulse.*

From this result, a startling difference can be seen between both time constants for both odors. Across the board, Benzaldehyde has lower values, indicating higher sensitivity towards the odor. This is the case as the time constants can be thought of as the speed at which the scent is acquired and released in the presence of a changing odor concentration. Further, it would make sense that the odor that the locust was less sensitive towards would evoke a lower response in the EAG would have longer acquisition and yield times, as the locust simply does not care as much about the odor. For the previous two results (**Figure 6 & Table 1**), there is high confidence in the validity of the results. This is the results were derived from the data provided. Further, the results between **Figure 6 & Table 1** back each other up, and make intuitive sense as explained above. Thus the confidence in the results for this section is high.

Finally, a linear model was built to predict the resulting EAG output for any given series of inputs. The model was build by producing a matrix ‘S’ where each row was a 5-second window of stimulus data. The subsequent rows are also a 5-second window of data; however, they are started at one time point past the start of the previous point window. This matrix is then coupled with an output vector ‘R,’ where each point in ‘R’ corresponds to the EAG response value at the final time point of the window in ‘S.’ From this

the relationship $k = S^{-1}R$ can be derived to solve the system of equations for a linear input-output model. The matrix 'S' and the vector 'R' were then generated in Matlab, and 'k' was solved for using the Matlab command 'pinv' to find the inverse of 'S.' This 'k' was then used to predict the EAG signal for a random series of input stimulus. A graph of 'k' and the predicted data EAG data is as follows:

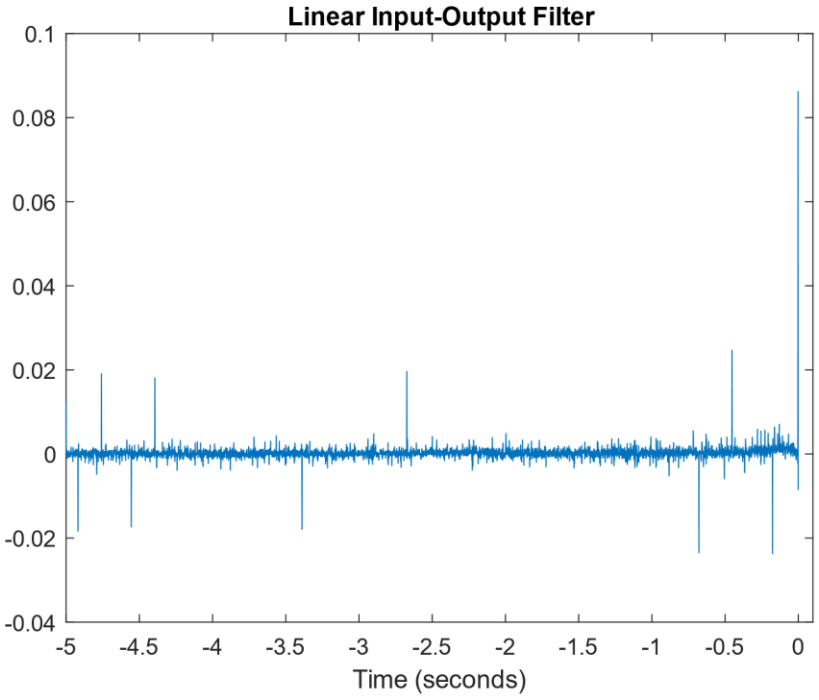

Figure 7: *This figure shows the linear filter 'k.' It can be seen that 'k' is essentially constant, with some noise, until the last 0.5 seconds. After this point, a slight bump and then a large spike is seen. The magnitude of 'k' is on the order of* 10^{-3} *for most of the time, and then 'k' spikes to be on the order of* 10^{-1} *for the very last few data points.*

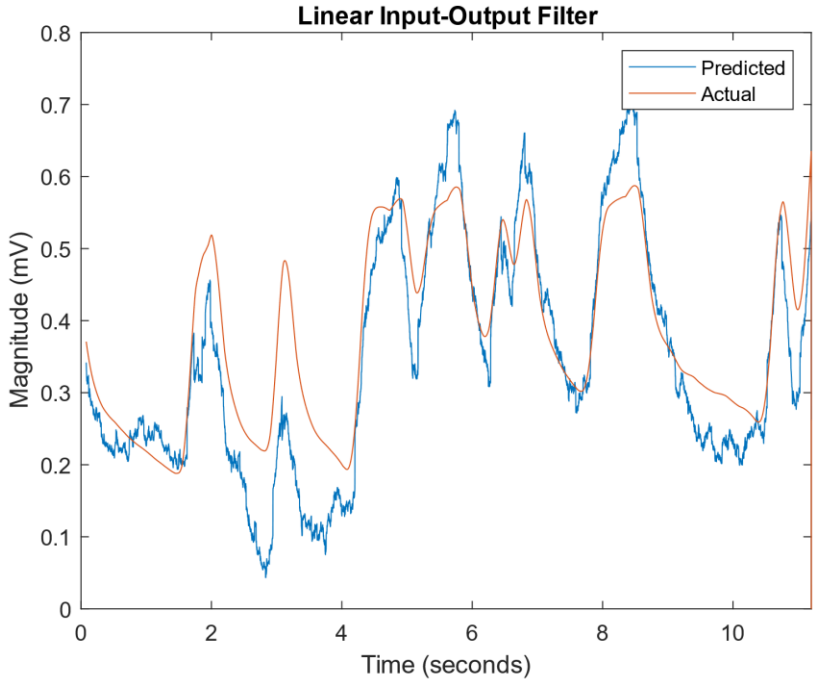

Figure 8: *This figure shows the filter 'k' from above used to predict the EAG response from an 'S' matrix generated on a testing data set. In the figure, the predicted signal is in blue, while the actual signal is in orange. The predicted EAG matches the general shape of the actual data; however, the specific magnitudes and nuances are not fully represented.*

From the result in **Figure 7,** it can be seen that the output is most influenced by the singular previous value of the signal. This is because of the large spike at t=0 in the plot of ‘k.’ This spike implies a large weighting to the most recent point of data in the input, which in this case is the similes signal. As the stimulation signal is represented by only 0s and 1s (0 = off and 1 = on), the most recent state of the stimulus is the most important. Furthermore, it appears as though stimuli from more than 0.5 seconds in the past hold, essentially no weight to the signal. This is indicative of a roughly 0.5-second temporal resolution for the response. I.e., the response is only dependent on what happened in the last 0.5 seconds of stimulus, and any longer timeframe has a negligible impact.

Using the calculated ‘k’ to predict a fit on another independent set of data, the results from **Figure 8** were generated. From this result, it can be seen that the prediction models the general trends of the actual data exceptionally well. However, it is far from perfect. The prediction is inconsistent with and quite poor at predicting specific amplitudes. Furthermore, the predicted fails to fully model the relative changes between the on and off signals, as well as the fact that the predicted data slightly lags the actual data. Thus, it can be said that the predicted model generated from ‘k’ is good for building an idea of the trend of the actual data, but is not useful for predicting nuances in the data.

For this final section, there is enough confidence in the results to display them; however, the confidence is not as strong as the confidence held in other portions of the lab. This is the case as although the data used is from the provided data, a differing selection of training data would lead to a different ‘k,’ which would lead to a slightly different prediction. Likewise, a different testing data set would also generate a differing prediction, and likely generate a differing goodness-of-fit of the prediction. Thus, there are too many variables that cannot be controlled, leading to a lack of strong confidence in the results. Furthermore, a conceptual or visual model for how or why ‘k’ looks the way it does is hard to build. It does make intuitive sense that the output response is influenced most by the most recent input; however, the specific shape that ‘k’ exhibits is hard to find intuitively, and thus cannot be easily validated logically.

Discussion:

From the results above, it can be fairly confidently stated that the amplitudes of the EAG response to both odors are not similar. The average amplitude for the hexanol data appears to be larger across both the 4-second pulse and the four tested ISI values. From the data in **Figure 6,** it can be seen that the EAG amplitude for benzaldehyde is consistently lower by roughly 0.18mV when compared to hexanol. These results make sense as we would not expect the two different odors to have identical responses from the locust, especially as these two odors are significantly different in terms of both molecular shape and natural source.

Likewise, not only are the EAG amplitudes not equal for both odors, the rise and fall time constants for both odors are not equal either. From the comparison in **Table 1**, it can be seen that both rise times and fall times for benzaldehyde are lower than the rise and fall times for hexanol. From this comparison, it can be inferred that the locust has greater specificity towards the benzaldehyde. This is the case as both the rise and fall times are lower, implying that the introduction of benzaldehyde triggers the antenna more quickly and sharply, while the removal of benzaldehyde likewise more quickly and sharply reduces antennal activity. This can be attributed to the fact that compounds like benzaldehyde are commonly found in plants and nature, which for locusts is their food. Thus, locusts would evolve to be more sensitive towards the compounds that mainly contribute to the smell of their food. This point is illustrated in *Nizampatnam et al., 2018,* where benzaldehyde is described as being an odor linked to the plants that the locusts eat, namely grass. Furthermore, in *Ito et al., 2008,* the locusts' preference for benzaldehyde is seen in the neural response from the odor and the lack of condition required for response to benzaldehyde.

Now that it is known that both odors elicit a differing response in both EAG amplitude and times constants, a discriminator for identifying which odor corresponds to a response in a scenario where the odor used is unknown. Thus, for this, the time constants will act as a much better discriminator between the two odors. This is the case as EAG amplitudes can change even across a recording session; however, rise and fall times should remain constant at least across recording sessions. Similarly, if the data is to be

generalized over numerous individual locusts, the EAG amplitudes would most definitely have significant variance, and the amplitude of hexanol may even exceed the amplitude of benzaldehyde. However, evolutionary preferences of the locust will remain, and the sensitivity towards benzaldehyde will continue to be expressed in the time constants.

Circling back to **Figures 2-5**, the temporal dynamics of the system can be teased apart. I.e., the temporal relationship between the stimulus and the EAG response can easily be seen, and any temporal discrepancies in the input-output relationship can be seen. These discrepancies can include anything from lagging responses to ignored stimuli. Thus looking into the temporal dynamics of the system, as reported by the EAG, it can be seen that the dynamics of the similes are represented quite well. From **Figures 2-5**, it can be seen that the voltage of the EAG responds in lockstep with the stimulus for all of the tested ISI values. However, the EAG response is not perfect. As the EAG is a population recording instead of a unit recording, the immediate response to a change in stimulus is lost as it is averaged across the population. However, this is relatively minor, and the EAG overall does a near-perfect job of representing the temporal dynamics of the stimulus.

Looking into the results drawn from varying ISI, an interesting phenomenon is seen; not only is the amplitude of the response decreasing as a function of decreasing ISI, but the amplitude is also decreasing at some nonlinear rate. The shape of this nonlinear decrease is quire reminiscent of exponential decay, as can be seen in **Figure 6**. When stimulation frequency increases (ISI decreases), the response amplitude decreases. This makes sense for a few reasons. First, as ISI decreases, the concentration of odor becomes greater, reducing the possible change from baseline that the ORNs in the antenna can produce, thus reducing the amplitude. Second, with lower ISIs, the odor concentration remains higher for longer, giving the ORNs in the antenna more time to adapt to the odor and thus reduce the activity caused by the odorant. Finally, as the ISI decreases, the time available for the antenna to return to resting voltage is

decreased, and thus when the next wave of activity hits the antenna, the peak is reached from the higher resting voltage, and thus, the amplitude is lower.

For the final part of the lab, the input-output filter, quite a lot can be gleaned from the results posted above. For example, the fact that the shape of the input-output filter that was generated is reminiscent of two shapes covered in class. First and foremost is an action potential, however, without the post-peak hyperpolarization. This can be seen in **Figure 7,** where it can be seen that the filter k appears to hover around a steady-state value, before a small bump that is then followed with a large peak, much like an action potential.

The second shape that the input-output filter is reminiscent of is that of a discrete-convolution lowpass filter. From what was taught by Dr. Barbour in module two of QP, a discrete-convolution lowpass filter can be represented with a rectangle, wherein the width of the rectangle corresponds to the cutoff frequency. From **Figure 8**, the rectangle can be seen by the large peak in the last few data points. Intuitively, it can be seen that the EAG output shape can be loosely modeled as a smoothed version of the stimulus. It is also known that a lowpass filter smooths the edges of a square wave signal as it removes the infinite frequency components of the rising and falling edges. Thus just from intuition, it can be seen that the input-output filter acts as a lowpass filter.

Conclusion:

From this lab, it has been shown that the locust has selectivity for certain odors over others, which in this case, was a selectivity for benzaldehyde over hexanol. This selectivity was shown in the difference of EAG amplitudes between the two odors. This selectivity was also shown to translate into increased sensitivity for the benzaldehyde over hexanol, shown via the decreased time constants for benzaldehyde. Following this, the effects of decreased ISI were shown. Specifically, the inverse relationship between

frequency and average amplitude of the response as recorded in the EAG data. Finally, a linear input-output filter was built using data collected from the lab. This linear filter was used to predict the output given a sequence of inputs. In this case, a filter that produced a fairly good representation of the actual output was generated. It is interesting to note that the filter resembled both an action potential and a lowpass filter in the discrete time-space. Further, it is seen that the output depends most heavily on the most recent stimulus value and that essentially all information from more than 0.5 seconds in the past is trivial to the output.

Through completing this lab, the principals of olfaction data collection and analysis have been thoroughly imparted to the students. Furthermore, the foundations of data modeling and prediction using linear models were established successfully in this lab. These concepts and tools successfully provide a basis for deeper study into olfaction within the field of biomedical engineering. Moreover, the lab has opened up the students to potential applications of olfaction and future avenues to expand into.

References:

1. Lab Partners: Bryce Maxwell, Whitaker Andrew
2. PLab Manual
3. Bio-Inspired Sensors, P. Wolf, American Physical Society, 2019
4. Breath analysis of cancer in the present and the future
5. Reef Einoch Amor, Morad K. Nakhleh, Orna Barash, Hossam Haick
6. European Respiratory Review Jun 2019, 28 (152) 190002
7. Scientists granted $750,000 to develop bomb-detecting locusts, D. Lugo, American Association for the Advancement of Science, 2016
8. Ito, I., Ong, R., Raman, B. et al. Sparse odor representation and olfactory learning. Nat Neurosci 11, 1177–1184 (2008)
9. Nizampatnam, S., Saha, D., Chandak, R. et al. Dynamic contrast enhancement and flexible odor codes. Nat Commun 9, 3062 (2018)

Unofficial References:

1. Other Individuals were consulted. However, there was no collaboration, only discussion
    a. Students are: Anthony Wu, Spencer Kaminsky, Precious Oluwakemi, Emily Ray
    b. Instructors include: Professor Widder, Professor Ledbetter